Catalysis Communications 53 (2014) 25–28

Contents lists available at ScienceDirect

Catalysis Communications

journal homepage: www.elsevier.com/locate/catcom

Short Communication

100% selective yield of *m*-nitroaniline by rutile TiO_2 and *m*-phenylenediamine by P25-TiO_2 during *m*-dinitrobenzene photoreduction

Jaspreet Kaur [1], Bonamali Pal *,[1]

School of Chemistry and Biochemistry, Thapar University, Patiala 147004, Punjab, India

ARTICLE INFO

Article history:
Received 20 January 2014
Received in revised form 28 March 2014
Accepted 24 April 2014
Available online 2 May 2014

Keywords:
Rutile-TiO_2 photoactivity
TiO_2 photocatalysis
Nitro to amino reduction
Dinitrobenzene photoreduction

ABSTRACT

Photoreduction of *m*-dinitrobenzene (25 μmol) in the deaerated aqueous iso-propanol exhibits 100% selective yield of *m*-nitroaniline (25 μmol) by rutile TiO_2 (50 mg) or *m*-phenylenediamine (25 μmol) by P25-TiO_2 separately under 8 and 4 h of UV light irradiation (125 W Hg arc, 10.4 mW/cm^2), respectively. It revealed that insertion of a second –NO_2 in nitrobenzene ring has an important role in expediting –NO_2 reduction to –NH_2 as compared to a negligible reduction of nitrobenzene under similar conditions, indicating that electron withdrawing groups lower the electron density on –NO_2 present on *meta* position and favor quick reduction of the –NO_2 group.

1. Introduction

The selective production of *m*-phenylenediamine (*m*-PDA) and *m*-nitroaniline (*m*-NA) derived from nitroaromatics reduction is very important for their use in pharmaceuticals, food additives, agrochemicals and dye products [1,2]. These are typically synthesized [3–6] by reduction of different nitroaromatics using Fe, Zn, Sn, Au–Ni alloy, Au/Pt-Al_2O_3, Pt/TiO_2, Fe_2O_3 and ZrO_2 etc. catalysts under harsh experimental conditions such as high pressure and temperature, toxic solvents and strong reducing agents like $NaBH_4$, where metal nanoparticles transfer the electron [7] from negatively charged BH_4^- to the nitro compound and thus leading to its reduction. Generally, reduction of *m*-dinitrobenzene (*m*-DNB) to *m*-PDA proceeds via the formation of *m*-NA, and the main challenge lies in the selective production of *m*-NA where the reduction [8,9] of both –NO_2 groups favorably produces *m*-PDA. Therefore, finding an effective catalytic process for the synthesis of *m*-NA or *m*-PDA from *m*-DNB under ambient conditions is of great industrial importance. Nitroorganic reduction by TiO_2 photocatalysis [10,11], a greener process is practically viable [12–14] because of the higher conduction band energy of TiO_2 (-0.85 V) relative to -0.5 V vs SCE of the –NO_2 group preferably reduced over aceto, cyano, and aldehyde functionality present in the same compound. It has been found that nitrobenzene (NB) generally reduced [15–17] to aniline, azoxybenzene and azobenzene by CdS, WO_3 and P25-TiO_2 under UV irradiation, whereas ZnO particles generate hydroxylamine [18], and core–shell SiO_2@Rh–CdS nanocomposites [19] produced 70% azoxybenzene under 436 nm light exposure. Therefore, activity/selectivity of nitroaromatics can be controlled by the choice of catalyst, its crystal phase, composition and suitable solvent. It revealed that partial reduction of one –NO_2 group of *m*-DNB to *m*-NA followed by subsequent reduction of the second –NO_2 group to *m*-PDA can limit the selectivity of P25-TiO_2 catalyst. Recently, rutile TiO_2 (R-TiO_2) has attracted much attention because of its superior ability for selective oxidation [20] of benzyl alcohol to benzaldehyde, *m*-nitrotoluene reduction [21] to *m*-aminotoluene, and other nitroorganic reduction [22,23] to aromatic amines. Thus, R-TiO_2 possessing low and slow reactivity could be effective for NA yield over PDA formation. Herein, we report that the photocatalytic reduction of *m*-DNB by R-TiO_2 in iso-propanol suspension led to 100% selective yield of *m*-NA for the first time in comparison to negligible activity for NB reduction, whereas, anatase–rutile mixed P25-TiO_2 produced 100% *m*-PDA yield under the same reaction conditions.

2. Experimental

2.1. Preparation, characterization and photocatalytic study of sintered TiO_2 samples

Commercial Degussa P25-TiO_2 was sintered at 400, 600 and 800 °C for 2 h to get the desired catalyst. Photoreduction was carried out in a test tube containing TiO_2 (50 mg) suspended in 5 ml (50%) of aqueous iso-propanol and NB, or *m*/*p*-DNB (25 μmol) using UV irradiation (125

---

* Corresponding author at: School of Chemistry and Biochemistry, Thapar University, Patiala-147001, Punjab, India.
E-mail address: bpal@thapar.edu (B. Pal).

[1] Tel.: +91 175 239 3128; fax: +91 175 236 4498.

http://dx.doi.org/10.1016/j.catcom.2014.04.019

W Hg arc, 10.4 mW/cm^2) under argon atmosphere and magnetic stirring. Reaction samples were analyzed by high performance liquid chromatography (HPLC) and gas chromatography–mass spectroscopy (GC–MS). The details of other characterizations of samples are given in supporting information.

3. Results and discussion

3.1. Structural analysis of catalysts

The rutile phase of sintered P25-TiO$_2$ was confirmed with XRD spectra as shown in Fig. 1 and the peaks at $2\theta = 27.5°$, $36.5°$, $41°$, $54.1°$, and $56.5°$ are assigned to its rutile phase. The fraction of rutile in each sample was calculated by using the Spurr equation [24]

$$\%\text{Rutile} = \frac{1}{1 + 0.8[I_A(101)/I_R(110)]}$$

where I_A is the intensity of the (101) peak and I_R is the intensity of the (110) peak. With the increase in sintering temperature from 400 to 800 °C, rutile content increases in P25-TiO$_2$ and pure (99.4%) R-TiO$_2$ sample was obtained at 800 °C. The BET surface area analysis exposed that the surface area decreases from 56 m^2 g^{-1} of P25-TiO$_2$ to 18 m^2 g^{-1} for pure R-TiO$_2$ with increased rutile content.

3.2. Photocatalytic activity of sintered P25-TiO$_2$ catalysts

The various solvents *viz*. methanol, ethanol and n-propanol have been tested for the photoreduction of *m*-DNB by R-TiO$_2$ under 8 h of UV light irradiation (Fig. 2a). Among various solvents, iso-propanol proved to be the best medium for 100% selective yield of *m*-NA, whereas, 46% *m*-PDA formation took place in ethanol solvent. It was reported that iso-propanol can be oxidized to acetone in a photocatalytic reaction, thus effecting the simultaneous reduction of the compound that is dissolved in it. Being a secondary alcohol, iso-propanol has a better hole scavenging capacity [6] than other primary alcohols and exhibits superior electron donating ability for the reduction process.

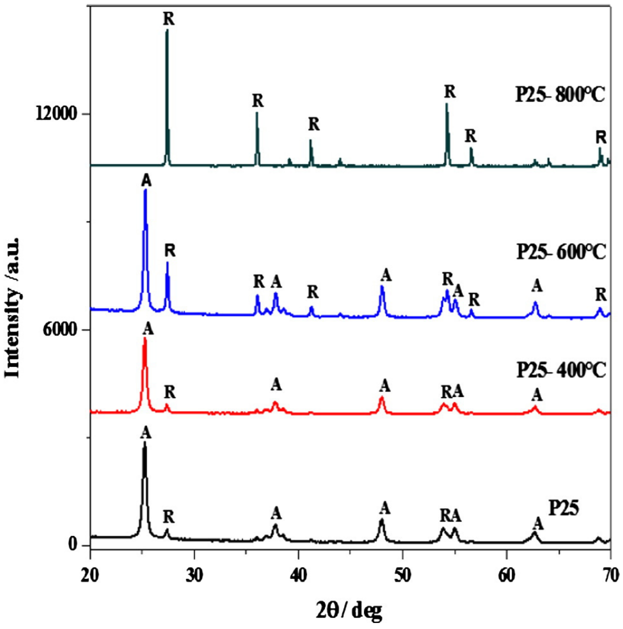

Fig. 1. XRD patterns of sintered P25-TiO$_2$ for 2 h at different temperatures.

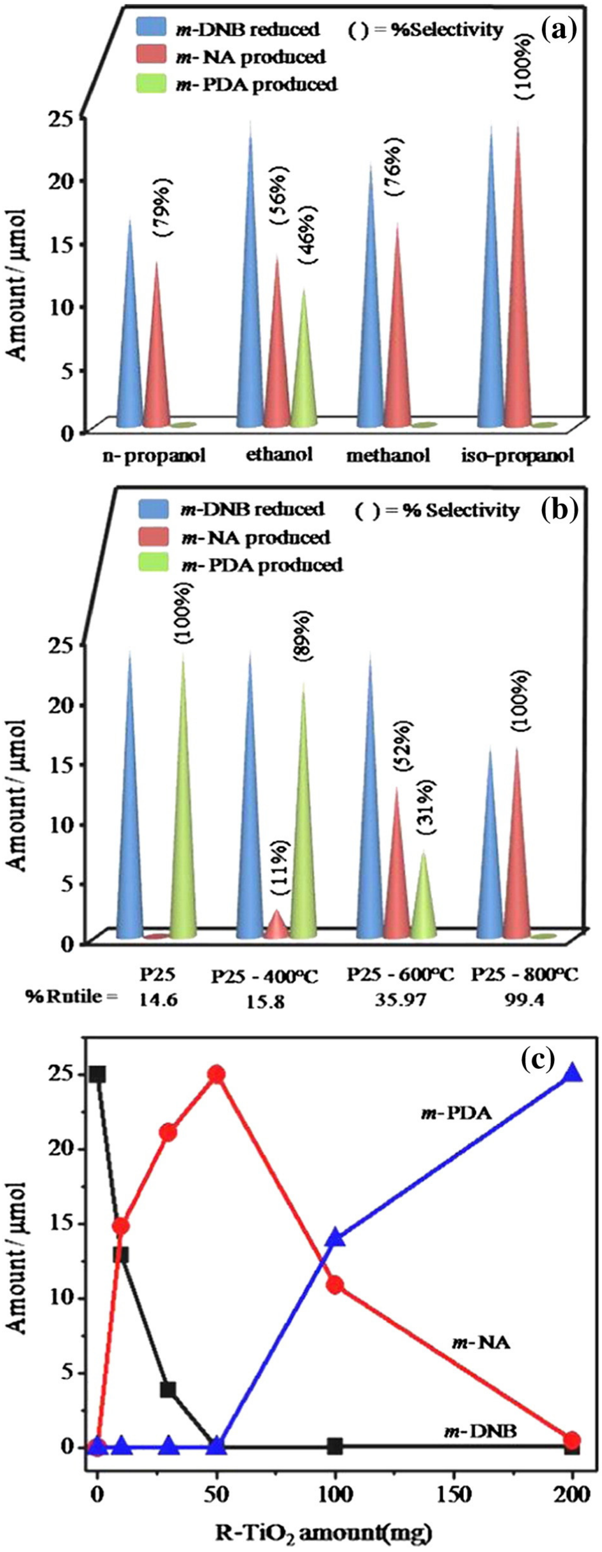

Fig. 2. *m*-DNB photoreduction (25 µmol) by (a) R-TiO$_2$ in different solvents under 8 h and (b) effect of R-TiO$_2$ content for 4 h and (c) amount of R-TiO$_2$ in iso-propanol for 8 h irradiation.

A comparative HPLC pattern (Fig. A1 in the supporting information) shows a clear separation of *m*-PDA ($t_R = 2.9$ min), *m*-NA ($t_R = 3.6$ min) and *m*-DNB ($t_R = 4.6$ min) peaks in a mixture (5 mM) of authentic samples, and *m*-DNB reduction by R-TiO$_2$ for 8 h irradiation displayed *m*-NA formation at $t_R = 3.6$ min and *m*-PDA at $t_R = 2.9$ min.

Fig. 2b showed that *m*-DNB (25 µmol) is selectively reduced to 100% *m*-PDA (25 µmol) by anatase–rutile mixed P25-TiO$_2$ catalyst and thereafter decreases with a gradual increase in *m*-NA yield as a function of increased rutile content, and reached to 100% *m*-NA yield by pure (99%) R-TiO_2 after 4 h UV irradiation.

The amount of *m*-DNB reduced is also subsequently decreased because of lower photoactivity of R-TiO_2. Fig. 2c demonstrated that *m*-NA yield is highly improved with the increased amount of R-TiO_2, and exhibits maximum *m*-NA yield by 50 mg catalyst, and beyond this amount, the second –NO_2 group of *m*-NA starts reducing to give *m*-PDA as a final product. This can be explained on the basis of increased per molecule interactions of *m*-DNB with increasing amount of R-TiO_2 and availability of a higher number of active Ti^{3+} sites that imparted in rapid reduction of both –NO_2 groups.

The amount of *m*-DNB is gradually reduced with an increased amount (17.9 μmol) of *m*-NA along with a little amount (3 μmol) of *m*-PDA produced by P25-TiO_2 during 2.5 h UV irradiation and, thereby, *m*-NA gets converted into 100% *m*-PDA (25 μmol) after 4 h light exposure (Fig. 3a). In contrary, complete reduction of *m*-DNB to *m*-NA by R-TiO_2 is clearly observed after 8 h reduction and thereafter irradiation (>8 h) led to less amount of *m*-PDA formation as shown in Fig. 3b. The efficiency of –NO_2 reduction to –NH_2 group is further verified by simultaneous analysis of acetone formed [11] during oxidation of iso-propanol under photoirradiation. It found that the amount of acetone formed is higher when both the –NO_2 groups are reduced to *m*-PDA than one –NO_2 reduction to *m*-NA formation as evident in the differences in peak area/height of acetone ($t_R = 1.2$ min) in the GC chromatogram (Fig. A2 in supporting information).

The GC–MS analysis revealed that a single sharp peak at $t_R = 5.5$ min (Fig. 3c) for *m*-PDA and at $t_R = 8.1$ min for *m*-NA (Fig. 3d) production by P25 and R-TiO_2 catalysts, respectively, evidencing cent percent yield and selectivity of the obtained products whose mass (Fig. 3e and f) fragmentation is also matched with the respective authentic samples, confirmed the purity of *m*-NA and *m*-PDA. Thus, it was found that *m*-DNB was efficiently and selectively reduced by the increased percentage of rutile content and reached to the highest rate by pure R-TiO_2 as compared to no appreciable reduction of NB under low intensity of UV light. These findings are little different from the selective reduction [21] of –NO_2 to –NH_2 group by R-TiO_2 particles (obtained from P25-TiO_2 with HF dissolution) using high power Xe lamp (2 kW, 27.3 W/m^2) illumination. This fact suggests that the substituent and the position of –NO_2 group on the NB ring have an important role in the reduction process because the electron withdrawing groups that lower the electron density on a –NO_2 group present on *meta* position favor the rapid conversion of the –NO_2 into the –NH_2 group and hence reduce the nucleophilicity of the resulting *m*-NA as observed in *m*-DNB reduction by P25-TiO_2. As the –NO_2 group in the *para* position imparted less electronic induction than the *meta* –NO_2 group, the selectivity of *p*-DNB (24 μmol) reduction to *p*-NA (17 μmol, 69%) is notably decreased without any production of *p*-PDA by R-TiO_2. This impact of –NO_2 substituent is further supported by the fact that almost no reduction (1–2 μmol) of NB to aniline (1 μmol) occurs by R-TiO_2 even after 8 h irradiation. However, P25-TiO_2 being its mixed anatase–rutile phase has higher catalytic activity; hence, 25 μmol *p*-DNB is reduced to 20 μmol *m*-PDA (82%) and 5 μmol *p*-NA (17%) relative to 14 μmol reduction of NB to 9 μmol aniline (66%) formation only after 4 h UV irradiation. It also observed that reduction of 25 μmol *m*-chloronitrobenzene by P25-TiO_2 gives 100% *m*-chloroaniline (25 μmol), whereas R-TiO_2 gives only 4 μmol of *m*-chloroaniline after 4 and 8 h light irradiation, respectively, probably because of the poor electron withdrawing nature of –Cl as compared to the –NO_2 group.

The measured surface area 56 $m^2\ g^{-1}$ of P25 is notably reduced with increased rutile content on increasing sintering temperature i.e., 38, 30 and 18 $m^2\ g^{-1}$ at 400, 600 and 800 °C, respectively. Therefore, although the *m*-DNB reduction rate is decreased from 6.25 to 3.12 μmol/h, the selectivity of *m*-NA yield is considerably improved because of the drastic changes in the surface electronic properties of R-TiO_2 with increased crystallinity [25] where fewer defect sites appeared to promote *m*-NA formation. The low photoreactivity of R-TiO_2 may probably be due to less surface OH concentration leading to poorer O_2 adsorption essentially required for proficient capturing of photoexcited electron [26–28] and hence, exhibits fast recombination of e^-/h^+ pairs relative to P25-TiO_2 catalyst. Many studies [20–29] have revealed that strong oxidation of TiO_2 at elevated temperatures leads to the formation of a metal-deficient oxide and predominant defects are oxygen vacancies that are important reactive agents for enhanced photocatalytic activity. The active sites for –NO_2 reduction on R-TiO_2 are the Ti^{3+} atoms [22,29] located at the oxygen vacancies on the R-TiO_2 surface which behave as

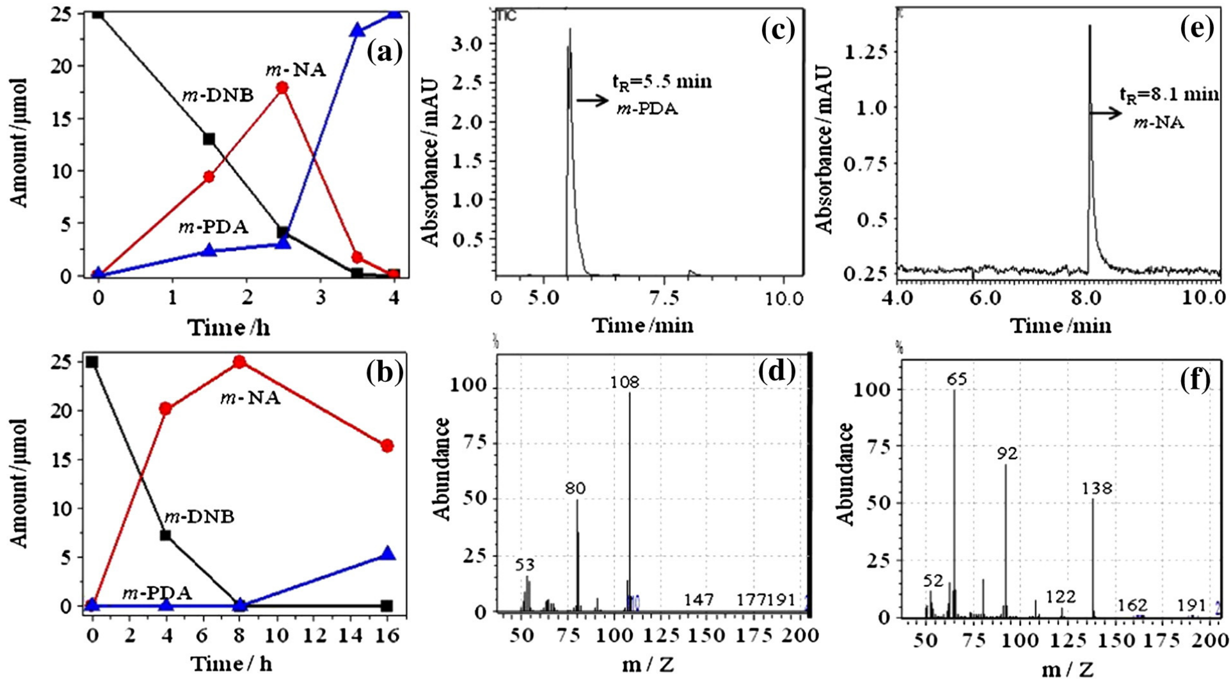

Fig. 3. Time course of *m*-DNB reduction by (a) P25-TiO_2 and (b) R-TiO_2 under UV irradiation, (c–d) and (e–f) chromatograph and mass spectra of *m*-PDA and *m*-NA formation by 4 h and 8 h photoreduction of *m*-DNB by P25-TiO2 and R-TiO_2 catalysts, respectively.

the adsorption site for DNB and the trapping site for conduction band electrons. Experimental results showed that R-TiO_2 particles possess {011} and {110} faces, and the anatase particles are exposed with {001} and {011} crystal faces, where the electronic energy levels of the {110} face are found to be lower than the {011} face helping the quick separation of photoexcited electrons and holes for the rutile [30,31] than anatase particles. This variation in the surface energy of the conduction and valence band of different crystal faces and their atomic arrangements thus affect the TiO_2 photoreactivity; hence facilitating the nitro-to-amine conversion by the surface-trapped electrons, enabling *m*-NA formation.

4. Conclusions

It is demonstrated that both the P25-TiO_2 and R-TiO_2 could be potentially utilized for the selective reduction of nitroaromatics possessing multifunctional reducible groups in *ortho*, *meta* and *para* position without any control of irradiation time. Thus, proper selection of electron donating or withdrawing substituent's in the aromatic moiety would be highly beneficial for several other products to obtain.

Acknowledgments

We are grateful to the Department of Science and Technology, India (SR/NM/NS-40/2008) for partial financial assistance. Special thanks to Dr. Satnam Singh and Inderpreet Singh Grover for surface area analysis.

Appendix A. Supplementary data

Supplementary data to this article can be found online at http://dx.doi.org/10.1016/j.catcom.2014.04.019. These data include MOL files and InChiKeys of the most important compounds described in this article.

References

[1] P.F. Vogt, J.J. Gerulis, Ullmann's Encyclopedia of Industrial Chemistry, Aromatic Amines, , Wiley-VCH, Verlag GmbH & Co. KGaA, Weinheim, 2005. 2.
[2] L. Yingxin, C. Jixiang, Z. Jiyan, Chin. J. Chem. Eng. 15 (2007) 63.
[3] F.C. Lizana, S.G. Quero, N. Perret, M.A. Keane, Catal. Lett. 127 (2009) 25.
[4] H. Rojas, G. Borda, P. Reyes, M. Brijaldo, J. Valencia, J. Chil. Chem. Soc. 56 (2011) 793.
[5] A. Corma, P. Serna, Science 313 (2006) 332.
[6] H. Zhu, X. Ke, X. Yang, S. Sarina, H. Liu, Angew. Chem. 122 (2010) 9851.
[7] S. Kundu, S. Lau, H. Liang, J. Phys. Chem. C 113 (2009) 5150.
[8] M.M. Telkar, J.M. Nadgeri, C.V. Rode, R.V. Chaudhari, Appl. Catal. A Gen. 295 (2005) 23.
[9] Y.X. Liu, J.X. Chen, J.Y. Zhang, Chin. J. Chem. Eng. 15 (2007) 63.
[10] F. Mahdavi, T.C. Bruton, Y. Li, J. Org. Chem. 58 (1993) 744.
[11] K. Imamura, T. Yoshikawa, K. Hashimoto, H. Kominami, Appl. Catal. B Environ. 134–135 (2013) 193.
[12] M.S. Wrighton, Chem. Eng. News 57 (1979) 29.
[13] M.A. Fox, Nouv. J. Chim. 11 (1987) 129.
[14] J.A. Dean, Handbook of Organic Chemistry, McGraw Hill, New York, 1987, (section 8).
[15] R.J. Tayade, R.G. Kulkarni, R.V. Jasra, Ind. Eng. Chem. Res. 45 (2006) 922.
[16] H. Wang, J. Yan, W. Chang, Z. Zhang, Catal. Commun. 10 (2009) 989.
[17] R.J. Tayade, D.L. Key, Mater. Sci. Forum 657 (2010) 62.
[18] Y. Li, L. Wang, in: P. Kamat, D. Meisel (Eds.), Nanocrystalline Semiconductor Materials, Elsevier, New York, 1996.
[19] B. Pal, T. Torimoto, K. Okazak, B. Ohtani, Chem. Commun. 5 (2007) 483.
[20] C.J. Li, G.R. Xua, B. Zhang, J.R. Gonga, Appl. Catal. B Environ. 115 (2012) 201.
[21] A. Hakki, R. Dillert, D.W. Bahnemann, Phys. Chem. Chem. Phys. 15 (2013) 2992.
[22] Y. Shiraishi, Y. Togawa, D. Tsukamoto, S. Tanaka, T. Hirai, ACS Catal. 2 (2012) 2475.
[23] S.C. Li, U. Diebold, J. Am. Chem. Soc. 132 (2010) 64.
[24] R.A. Spurr, H. Myers, Anal. Chem. 29 (1957) 760.
[25] S. Yurdakal, G. Palmisano, V. Loddo, O. Alagoz, V. Augugliaro, L. Palmisano, Green Chem. 11 (2009) 510.
[26] A. Kudo, Y. Miseki, Chem. Soc. Rev. 38 (2009) 253.
[27] K. Kobayatawa, Y. Nakazawa, M. Ikada, Y. Sato, A. Fujshima, Ber. Bunsenges. Phys. Chem. 94 (1990) 1439.
[28] R. Campostrini, G. Carturan, L. Palmisano, M. Schiavello, A. Sclafani, Mater. Chem. Phys. 38 (1994) 277.
[29] S. Yin, H. Hasegawa, D. Maeda, M. Ishitsuka, T. Sato, J. Photochem. Photobiol. A Chem. 163 (2004) 1.
[30] T. Ohno, K. Sarukawa, M. Matsumura, New J. Chem. 26 (2002) 1167.
[31] Y. Aoyama, Y. Oaki, R. Ise, H. Imai, Cryst. Eng. Comm. 14 (2012) 1405.